NUCLEAR SCIENCE AND ENGINEERING: **128**, 186–208 (1998)

# Automated Variance Reduction of Monte Carlo Shielding Calculations Using the Discrete Ordinates Adjoint Function

John C. Wagner* and Alireza Haghighat

*The Pennsylvania State University, Department of Nuclear Engineering*
*231 Sackett Building, University Park, Pennsylvania 16802*

*Received December 12, 1996*
*Accepted July 22, 1997*

**Abstract**—*Although the Monte Carlo method is considered to be the most accurate method available for solving radiation transport problems, its applicability is limited by its computational expense. Thus, biasing techniques, which require intuition, guesswork, and iterations involving manual adjustments, are employed to make reactor shielding calculations feasible. To overcome this difficulty, we have developed a method for using the $S_N$ adjoint function for automated variance reduction of Monte Carlo calculations through source biasing and consistent transport biasing with the weight window technique. We describe the implementation of this method into the standard production Monte Carlo code MCNP and its application to a realistic calculation, namely, the reactor cavity dosimetry calculation. The computational effectiveness of the method, as demonstrated through the increase in calculational efficiency, is demonstrated and quantified. Important issues associated with this method and its efficient use are addressed and analyzed. Additional benefits in terms of the reduction in time and effort required of the user are difficult to quantify but are possibly as important as the computational efficiency. In general, the automated variance reduction method presented is capable of increases in computational performance on the order of thousands, while at the same time significantly reducing the current requirements for user experience, time, and effort. Therefore, this method can substantially increase the applicability and reliability of Monte Carlo for large, real-world shielding applications.*

## I. INTRODUCTION

In the field of nuclear engineering, deterministic (discrete ordinates) and stochastic (Monte Carlo) methods are most often used to solve shielding-type problems. As one might expect, each method has its own strengths and weaknesses. In general, Monte Carlo methods are more accurate, but they require far greater computational resources. This is particularly true for deep-penetration shielding calculations involving attenuation of several orders of magnitude. Despite the steady increase in available computational performance, unbiased or analog Monte Carlo methods are not practical, or even possible, for real reactor shielding applications. For these applications, either biased Monte Carlo methods or the discrete ordinates ($S_N$) method is used; however, the latter contains uncertainties associated with the discretization of the independent variables of the transport equation. In this work, we take advantage of the strengths of both methods and use them in a complementary manner. Specifically, we have developed a method for using the $S_N$ adjoint function for automatic variance reduction of Monte Carlo calculations through source biasing and consistent transport biasing with the weight window technique.

### *I.A. Motivation*

The Monte Carlo method is considered to be the most accurate method presently available for solving radiation transport problems. However, because of its very nature of simulating individual particles and inferring the average behavior of the particles in the system from the average behavior of the individually simulated particles, it is extremely expensive computationally. In fact, for many reactor applications, as well as medical and nuclear-well-logging applications, the computer time required by

*Current address: Holtec International, 555 Lincoln Drive West, Marlton, New Jersey 08053.

the analog Monte Carlo method is prohibitive and/or impractical. As a simple example, consider a problem in which the transmission probability is $10^{-8}$. If we assume that 1000 particle histories can be simulated per second, we can approximate that $\sim 6.7 \times 10^5$ min, or 1.3 yr, of CPU time would be required to reach an acceptable $1\sigma$ statistical uncertainty of 5%. If we further assume that we have exclusive access to a large enough number of computer processors to achieve a factor of 100 speedup, this calculation would still require nearly 5 days. Therefore, for difficult shielding problems in which the probability is small that a particle will contribute to the detector of interest, some form of variance reduction or biasing must be applied. Herein, the expressions *variance reduction* and *biasing* refer to fair-game techniques used in Monte Carlo calculations to reduce the computer time required to obtain results of sufficient precision.

To make a difficult Monte Carlo shielding calculation computationally practical or, in most cases, possible, we employ our basic knowledge of the physics of the problem and the available variance reduction techniques to coerce important particles to contribute to the quantity of interest (e.g., reaction rate, dose, etc.). While the application of variance reduction techniques is fairly straightforward for simple one-dimensional problems, it can be quite difficult for realistic problems, which are often complex and three-dimensional. Thus, the shielding analyst typically engages in an iterative process to develop the variance reduction parameters and subdivide the geometry to facilitate the parameters, converging at some acceptable level of calculational efficiency. Unfortunately, the appropriate variance reduction parameters vary significantly with problem type and objective. Therefore, the iterative steps must be repeated to determine the variance reduction parameters for calculations with different objectives (even for the same problem).

A further difficulty lies in the statistical convergence of the Monte Carlo results. For large, complex applications, it is not uncommon to spend days (and possibly weeks, depending on the problem, the user's experience, and the desired precision) iterating and adjusting the variance reduction parameters, only to achieve reasonable efficiency with unstable statistical behavior. This unstable statistical behavior is caused by improper use of the variance reduction methods (i.e., insufficient detail and/or inappropriate selection of the parameters) and is usually the result of undersampling some important region of the problem phase-space.[1] Further, this undersampling is often difficult to identify and correct.

### *I.B. Review of the Literature*

Over the past several decades, a large number of techniques have been developed to reduce the variance or increase the efficiency of Monte Carlo calculations.[2–6] These techniques were formulated with the premise that the importance of particles (important function) with respect to the calculational objective was known. All of these techniques modify the physical laws of radiation transport in an attempt to sample more particles in regions of the phase-space that contribute to the objective (i.e., detector). To compensate for this departure from the physical laws of radiation transport, the concept of particle weight ($w$) is introduced, where the weight can be considered as the number of particles being transported. When a variance reduction technique is applied, the weight of the particle is adjusted using the following "conservation" formula:

$$w\,[\text{biased probability density function (pdf)}] = w_0\,(\text{unbiased pdf})\ , \tag{1}$$

where $w_0$ is the weight before the variance reduction technique is applied. Therefore, nonanalog Monte Carlo is acceptable (i.e., it produces correct, unbiased estimates) as long as the particle weights are conserved. For example, in the implicit capture technique, a particle always survives a collision, but the particle emerges from the collision with a weight that has been reduced by a factor $(\sigma_s/\sigma_t)$, which is the probability of scattering. Thus, the total particle weight is conserved.

While some of these techniques, such as splitting/roulette and implicit capture, have widespread applicability, others, such as the exponential transformation and forced collisions, have been developed for particular classes of problems. Nevertheless, these techniques and many others are available in the standard production Monte Carlo codes, such as MCNP (Ref. 7), MORSE (Ref. 8), MCBEND (Ref. 9), and TRIPOLI (Ref. 10).

The biasing schemes for Monte Carlo particle transport can be divided into three major categories: source biasing, transport biasing (e.g., splitting/roulette and exponential transformation), and collision biasing (e.g., discrete-angle biasing, forced collisions, and implicit capture). As the names suggest, the three methods bias the source-sampling, transport, and collision processes, respectively. Of these methods, the transport-biasing method of splitting/roulette has been the most important method for increasing the efficiency of Monte Carlo calculations in general.[2,7]

As mentioned, all of the techniques require problem-specific parameters that are dependent on the importance of particles with respect to the objective function and are therefore difficult to use. Booth and Hendricks[11] state, "The selection [of parameters] is more art than science, and typically, the user makes a few short trial runs and uses the information these trials provide to better guess the parameters; that is, the user learns to adjust parameters on the basis of previous experience."

Responding to this difficulty, a number of strategies for determining variance reduction parameters based on the concept of learning were proposed and developed. MacDonald[13] demonstrated that through the use of pattern

recognition techniques, the Monte Carlo splitting surfaces could be learned. The learning mechanics were quite involved, and the method worked with very limited success on complicated geometries. Deutsch and Carter[13] showed that importances could be estimated at geometry surfaces during a forward Monte Carlo calculation and subsequently used to assist the analyst in manually selecting the various variance reduction parameters. Goldstein and Greenspan[14] developed a recursive Monte Carlo (RMC) method for estimating the importance function distribution. The method involved extensively subdividing the geometric regions and solving the forward problem for region importances with varying degrees of accuracy. While this work was reasonably successful, it was concluded that for deep-penetration problems to be efficient, the relevant importance function distribution must be known with sufficient accuracy; insufficient accuracy can lead to significant errors in the prediction of the detector response. Further, Goldstein and Greenspan concluded that it is far better to invest more time in the importance estimation calculation (the RMC calculation) than in the detector response calculation.

Continuing along these lines, Booth[15] and Booth and Hendricks[11] developed an importance estimation technique called the forward-adjoint generator, which has since become known as the weight window generator[16] because it estimates importances to be used with the weight window technique. The weight window technique, which is available in the standard version of MCNP, is simply a space- and energy-dependent facility by which splitting and Russian roulette are applied. The importance is estimated as the ratio of the total score due to particles (and their progeny) entering a cell to the total weight entering a cell, in a forward Monte Carlo calculation.

Independently, another stochastic optimization method, the direct statistical approach (DSA), was introduced by Dubi, Elperin, and Dudziak[17] and Dubi, Gugvitz, and Burn[18] and later extended by Burn.[19,20] In the DSA, expressions for the dependence of the second moment and the calculation time on the splitting parameters are derived. From these expressions and initial "learning" calculations to estimate the second moment and time function, splitting parameters may be optimized.

These approaches to estimating importances are basic to the forward-learning Monte Carlo methods, and therein lies the fundamental problem. To accurately estimate the importance of a space-energy interval, a sufficient number of particles must pass through that space-energy interval and proceed to contribute to the objective. In practice, this condition is typically not met, and as a result, either no importance estimate or an unreliable importance estimate is generated for each space-energy interval. Therefore, current forward Monte Carlo importance generators, such as the weight window generator, are restricted by their statistical nature and are of limited use in multidimensional deep-penetration problems. In the absence of more sophisticated methods, however, the weight window generator is a very useful tool in the iterative process of determining the variance reduction parameters.[11,21]

Therefore, it is apparent that a deterministic means of generating problem-dependent importances would be very beneficial for applying the Monte Carlo method to large/complex problems. It has long been recognized that the adjoint function (i.e., the solution to the adjoint Boltzmann transport equation) has physical significance as a measure of the importance of a particle to some objective function (e.g., the response of a detector).[22] It is this physical interpretation that, in theory, makes the adjoint function well suited for use as an importance function for biasing Monte Carlo calculations.

Coveyou, Cain, and Yost[23] developed an inverse relation between particle statistical weight and the adjoint (importance) function and showed the merits of the importance function for transport and source biasing. Kalos[24] described the importance-sampling technique and its relation to an importance function and a zero-variance solution. Following these works, a number of applications of deterministic and approximate adjoint solutions were made with varying degrees of success.[25–37] Tang, Stevens, and Hoffman[27] applied the one-dimensional $S_N$ adjoint solution to biasing shipping-cask calculations with MORSE. Miller et al.[29] developed an automatic importance generator for geometric splitting based on diffusion calculations and have incorporated it into the MCBEND code. Mickael[31,32] developed a version of MCNP that performs an adjoint diffusion calculation to generate weight window parameters for nuclear-well-logging calculations. Turner[36] has described the local importance function transform method, which uses a deterministic adjoint to bias distance-to-collision and selection of postcollision energy group and direction for multigroup Monte Carlo calculations. Recently, Van Riper et al. have developed the AVATAR method,[37] which uses the basic inverse relation between statistical weight and importance to calculate space-, energy-, and angular-dependent weight windows from a three-dimensional adjoint calculation.

Thus, the idea of using the adjoint (importance) function for variance reduction of Monte Carlo calculations is not new. However, several issues related to obtaining and using the adjoint function remain. Specifically, previous work has not precisely accounted for the inherent coupling between source and transport biasing, and most have required predefined spatial meshes for the Monte Carlo calculations and thus have focused on specific problem types.

In this work, we propose a method for using the $S_N$ adjoint function for automatic variance reduction of Monte Carlo calculations through source biasing and consistent transport biasing with the weight window technique. We deviate from the standard inverse relation and use the concept of importance sampling to derive consistent relations for source-biasing parameters and weight window lower bounds. For brevity, we refer to this method as CADIS (consistent adjoint driven importance sampling).

Source biasing is extremely important because (a) it is very effective in reducing the variance, and (b) it allows us to derive equations for the source-biasing parameters and weight window lower bounds such that the particles are produced with corresponding weights within the weight window intervals. Previous methods, such as AVATAR, which use the inverse of the adjoint function normalized to a particular (or average) source location and energy, do not account for the inherent coupling between source and transport biasing. Further, they do not take full advantage of the adjoint function via source biasing. As a result, these methods are not effective for problems containing highly distributed sources, such as most reactor shielding problems, in which the adjoint function can vary by several orders of magnitude within the source region. They are, however, effective for problems characterized by point-type sources (e.g., monoenergetic point source), such as nuclear-well-logging problems.

We describe the implementation of CADIS into the standard production Monte Carlo code MCNP and its application to a realistic calculation, namely the reactor cavity dosimetry calculation. The effectiveness of the method, as demonstrated through the increase in calculational efficiency, is demonstrated and quantified. Moreover, this paper addresses important issues associated with this procedure and its efficient use and implementation.

The CADIS method has the following desirable features:

1. It is based on the source-biasing and weight window techniques, which are statistically stable and generally applicable.

2. It does not in any way restrict the accuracy of the explicit three-dimensional continuous energy and angular Monte Carlo method.

3. Because of its practicality, stability, and general applicability, this method may be used for complete automation when coupled to an $S_N$ adjoint generator.

4. The method requires little or no experience on the part of the user.

This paper is organized as follows: The theory behind the CADIS method is presented in Sec. II. The implementation of this method into MCNP is described in Sec. III. Analysis related to the application and computational benefits of the CADIS method for a one-dimensional test problem and a real-world application are discussed in Sec. IV. The effect of adjoint energy and spatial accuracy on calculational efficiency is examined in Sec. V. Section VI summarizes and draws conclusions on this work, and finally, recent developments are reported in Sec. VII.

## II. THEORY

Problems that can be solved by the Monte Carlo method are essentially equivalent to integrations.[2] For example, the goal of most Monte Carlo particle transport problems is to calculate the response (i.e., flux, dose, reaction rate, etc.) at some location. This is equivalent to solving the following integral:

$$R = \int_P \Psi(P)\sigma_d(P)\,dP \quad , \tag{2}$$

where $\Psi$ is the particle flux and $\sigma_d$ is some objective function in phase-space $(r, E, \hat{\Omega}) \in P$.

From the following adjoint identity,[22]

$$\langle \Psi^\dagger H \Psi \rangle = \langle \Psi H^\dagger \Psi^\dagger \rangle \quad , \tag{3}$$

where $H^\dagger$ is the adjoint operator and $\langle\ \rangle$ signify integration over all the independent variables, one can show that the response $R$ (for a vacuum boundary condition) is also given by

$$R = \int_P \Psi^\dagger(P) q(P)\,dP \quad , \tag{4}$$

where $\Psi^\dagger$ and $q$ are the adjoint function and source density, respectively, and Eqs. (2) and (4) are equivalent expressions for $R$. The function $\Psi^\dagger(P)$ has physical meaning as the expected contribution to the response $R$ from a particle in phase-space $P$, or, in other words, the importance of a particle to the response.

To solve this integral with the Monte Carlo method, the independent variables are sampled from $q(P)$, which is not necessarily the best pdf from which to sample. An alternative pdf $\hat{q}(P)$ can be introduced into the integral as follows:

$$R = \int_P \left[ \frac{\Psi^\dagger(P) q(P)}{\hat{q}(P)} \right] \hat{q}(P)\,dP \quad , \tag{5}$$

where $\hat{q}(P) \geq 0$ and $\int_P \hat{q}(P)\,dP = 1$.

From importance sampling,[4] the alternative pdf $\hat{q}(P)$ that will minimize the variance for $R$ is then given by

$$\hat{q}(P) = \frac{\Psi^\dagger(P) q(P)}{\int_P \Psi^\dagger(P) q(P)\,dP} \quad . \tag{6}$$

If the final result $R$ is known, then the Monte Carlo integration will return $R$ with zero variance. However, in practice, the adjoint function is not known exactly, $R$ cannot be solved for by direct integration, and thus, it is necessary to simulate the particle transport. For this process, it is desirable to use the biased source distribution in Eq. (6) that, in the limit of an exact adjoint, leads to a zero-variance solution.

Examining Eq. (6) reveals that the numerator is the detector response from phase-space $P$, and the denominator is the total detector response $R$. Therefore, the ratio is a measure of the contribution from phase-space $P$ to the detector response. Intuitively, it is useful to bias the

sampling of source particles by the ratio of their contribution to the detector response, and therefore, this expression could also be derived from physical arguments.

Because the source variables are sampled from a biased pdf, the statistical weight of the source particles must be corrected according to Eq. (1) such that

$$W(P)\hat{q}(P) = W_0 q(P) \ , \tag{7}$$

where $W_0$ is the unbiased particle starting weight, which is set equal to 1. Substituting Eq. (6) into Eq. (7) and rearranging, we obtain the following expression for the statistical weight of the particles:

$$W(P) = \frac{\int_P \Psi^\dagger(P) q(P)\, dP}{\Psi^\dagger(P)} = \frac{R}{\Psi^\dagger(P)} \ . \tag{8}$$

This equation shows an inverse relationship between the adjoint (importance) function and the statistical weight. Previous work[23] in this area assumed this relationship and showed it to be near optimal, and others have verified this relationship through computational analysis.[27,38] However, in this work, beginning with importance sampling, we have derived (not assumed) this relationship.

To consider the transport process, we examine the integral Boltzmann transport equation for particle density in the phase-space $P$, given by

$$\Psi(P) = \int K(P' \to P)\Psi(P')\, dP' + q(P) \ , \tag{9}$$

where $K(P' \to P)\, dP$ is the expected number of particles emerging in $dP$ about $P$ from an event in $P'$, and $q(P)$ is the source density. To transform Eq. (9) to be in terms of the biased source distribution $\hat{q}(P)$, we multiply it by

$$\frac{\Psi^\dagger(P)}{\int \Psi^\dagger(P) q(P)\, dP} \tag{10}$$

and define

$$\hat{\Psi}(P) = \frac{\Psi(P)\Psi^\dagger(P)}{\int \Psi^\dagger(P) q(P)\, dP} \tag{11}$$

to yield the following transformed equation:

$$\hat{\Psi}(P) = \int K(P' \to P)\Psi(P')\, dP' \times \frac{\Psi^\dagger(P)}{\int \Psi^\dagger(P) q(P)\, dP} + \hat{q}(P) \ , \tag{12}$$

or

$$\hat{\Psi}(P) = \int K(P' \to P)\hat{\Psi}(P')\left[\frac{\Psi^\dagger(P)}{\Psi^\dagger(P')}\right] dP' + \hat{q}(P) \ . \tag{13}$$

This transformed equation can be written as

$$\hat{\Psi}(P) = \int \hat{K}(P' \to P)\hat{\Psi}(P')\, dP' + \hat{q}(P) \ , \tag{14}$$

where

$$\hat{K}(P' \to P) = K(P' \to P)\left[\frac{\Psi^\dagger(P)}{\Psi^\dagger(P')}\right] \ . \tag{15}$$

Because $K(P' \to P)$ is not known, we simulate the particle transport between events in the normal (unbiased) way and alter the number of particles emerging in $P$ from an event in $P'$ by the ratio $\Psi^\dagger(P)/\Psi^\dagger(P')$, which is the ratio of importances. This adjustment to the transfer kernel can be accomplished through particle creation and termination, such that

$$\text{for } \frac{\Psi^\dagger(P)}{\Psi^\dagger(P')} > 1 \ , \quad \text{particles are created (splitting)} \ , \tag{16}$$

and

$$\text{for } \frac{\Psi^\dagger(P)}{\Psi^\dagger(P')} < 1 \ , \quad \text{particles are destroyed (roulette)} \ . \tag{17}$$

Because we are altering the number of particles emerging from an event, the statistical weight of the particles must be corrected according to the conservation relation of Eq. (1) such that

$$W(P)K(P' \to P)\left[\frac{\Psi^\dagger(P)}{\Psi^\dagger(P')}\right] = W(P')K(P' \to P) \ , \tag{18}$$

or

$$W(P) = W(P')\,\frac{\Psi^\dagger(P')}{\Psi^\dagger(P)} \ . \tag{19}$$

While the development of the equations is based on the concept of zero variance, a zero variance cannot be attained with estimation at particle events (e.g., collision, boundary crossings, etc.) because the number of events is itself a random variable and contributes to the variance of the final result. However, reduced variance (even zero-variance solutions in the limit) can be achieved when every sampling (source and transport) is made proportional to its importance.

To administer the splitting and rouletting of particles, we use the weight window technique available within MCNP, which deals with particle weights. We have related the weights to particle importance via Eqs. (8) and (19). Because these relationships for the particle statistical weights, which are used in source sampling and the particle transport process, were derived from importance sampling in a consistent manner, we refer to the use of the relations as consistent adjoint driven importance sampling (CADIS).

## III. IMPLEMENTATION INTO MCNP

In Sec. II, we defined expressions for the source-biasing parameters and weight window lower bounds based on the adjoint (importance) function. In this section, we describe how this information is used within MCNP, and we discuss the related difficulties and issues.

### *III.A. Calculation of Variance Reduction Parameters*

To calculate source-biasing parameters over the phase-space (space, energy, and angle), the source from the forward calculation is coupled with the adjoint function as shown in Eq. (6). Further, the particle transport is biased via Eqs. (8) and (19).

The space-, energy-, and angular-dependent adjoint function may require a significant amount of storage, particularly for large three-dimensional problems. The $S_N$ method can determine the scalar (angular-independent) adjoint accurately, but not necessarily the angular-dependent adjoint because of the limited number of directions. Therefore, because of the memory requirements and inaccuracies of the angular-dependent adjoint, we use the space- and energy-dependent (scalar) adjoint function

$$\phi^\dagger(r,E) = \int_{4\pi} \Psi^\dagger(r,E,\hat{\Omega})\, d\hat{\Omega} \tag{20}$$

for calculating space- and energy-dependent source-biasing and weight window parameters. It should be noted, however, that the use of a less accurate adjoint (importance) function may reduce the efficiency (with respect to that from a very accurate adjoint function) but does not impact the accuracy of the Monte Carlo result.

#### III.A.1. Source Biasing

Source biasing allows the simulation of a larger number of source particles, with appropriately reduced weights, in the more important regions of each variable (e.g., space, energy, and angle). This technique consists of sampling the source from a biased (nonanalog) probability distribution rather than from the true (analog) probability distribution and then correcting the weight of the source particles by the ratio of the actual probability divided by the biased probability according to Eq. (1). Thus, the total weight of particles started in any given interval is conserved, and an unbiased estimate is preserved.

The source energy and position are sampled from the following biased source distribution

$$\hat{q}(r,E) = \frac{\phi^\dagger(r,E)q(r,E)}{\int_V \int_E \phi^\dagger(r,E)q(r,E)\, dr\, dE} = \frac{\phi^\dagger(r,E)q(r,E)}{R} \quad . \tag{21}$$

To calculate the source-biasing parameters from this relation, it is necessary to couple the $S_N$ adjoint function and the forward Monte Carlo problem description. Physically, the numerator is the detector response from space-energy element $(dr, dE)$, and the denominator is the total detector response $R$. Therefore, the ratio is a measure of the relative contribution to the detector response.

#### III.A.2. Transport Biasing

As mentioned, the weight window, as implemented in the MCNP code, is a space- and energy-dependent technique by which splitting/roulette are applied. The weight window technique provides an alternative to geometric splitting/roulette and energy splitting/roulette for assigning space- and energy-dependent importances. To use the weight window technique within MCNP, we need to calculate weight window lower bounds $W_l$ such that the statistical weights defined in Eq. (8) are at the center of the weight windows (intervals). The width of the interval is controlled by the parameter $C_u$, which is the ratio of upper and lower weight window values ($C_u = W_u/W_l$). Therefore, the space- and energy-dependent weight window lower bounds $W_l$ are given by

$$W_l(r,E) = \frac{W}{\left(\frac{C_u+1}{2}\right)} = \frac{R}{\phi^\dagger(r,E)} \frac{1}{\left(\frac{C_u+1}{2}\right)} \quad , \tag{22}$$

and during the transport process, the weight window technique performs splitting or roulette in a manner consistent with Eq. (19).

It is important to note that because the source-biasing parameters and weight window lower bounds are consistent, the statistical weights of the source particles $[W(r,E) = q(r,E)/\hat{q}(r,E)]$ are within the weight windows as desired. Moreover, if the statistical weights of the source particles are not within the weight windows, the particles will immediately be split or rouletted in an effort to bring their weights into the weight windows.[7] This will result in unnecessary splitting/rouletting and a corresponding degradation in computational efficiency. For problems in which the adjoint function varies significantly within the source region (space and/or energy),

this coupling between source and transport biasing is critical.

### *III.B. Integration of Importance Function into MCNP*

The general version of MCNP provides facilities for energy- and cell-dependent weight windows. This means that in order to use a fine spatial weight window grid (which is necessary in optically thick regions) with the standard version of MCNP, the user must subdivide the MCNP-cell–based geometry such that the ratio of importances between adjacent geometric cells is not too large. Because the importance ratios are not a priori known, this geometric discretization is not straightforward and typically requires iterations of manual adjustments. Further, the subdivision of the geometry into a very large number of cells is time-consuming and can actually degrade the efficiency of the calculation. For these reasons, we use the deterministic $S_N$ spatial mesh description to construct a separate, but related, geometric grid to facilitate the use of the adjoint distribution. This is done with a modified version of the MCNP code that is able to read the binary flux file (which contains the adjoint function and the spatial mesh and energy group information) from the standard $S_N$ DORT code[39] and superimpose the variable spatial mesh and energy grid onto the MCNP problem in a manner transparent to the user. This grid enables the use of the space- and energy-dependent importance function and does not directly affect the transport of particles. At various events in a particle history (e.g., collisions, surface crossings, and/or increments of mean free path), the grid is searched to determine the importance of the phase-space within which the particle resides. The importance is then compared to the statistical weight of the particle and the appropriate action is taken (e.g., splitting, Russian roulette, or no action). It should be noted that with the cell-based weight windows in the standard version of MCNP, additional spatial searching is not required.

Currently, the level of detail of the energy-dependent importance function is dictated by the multigroup library used for the $S_N$ adjoint calculation (i.e., all groups are used). The effect on the calculational efficiency of using fewer groups is discussed in Sec. V.

### *III.C. Weight Checking*

Various concepts for minimizing the amount of computational overhead associated with this process have been examined. The first issue of concern is the determination of the appropriate occasion (or event) to check the particle's statistical weight. Because the MCNP geometry does not need to be manually subdivided to assign the spatial importances, the presently available weight checks (i.e., at collisions and surface crossings) are no longer sufficient to control particle weight, and thus, large differences in the weight scored by individual particles are possible. Additional (more frequent) weight checking has two competing effects: (a) There is a computational cost or penalty each time the weight is checked, and this penalty is the time required by the searching routines to determine the importance of the phase-space within which the particle resides; and (b) more frequent checking leads to more reliable results with well-behaved statistical convergence. Therefore, it is clear that we need to determine a criterion for an optimum or near-optimum compromise for checking particle statistical weights. Moreover, it is desirable that this criterion be problem independent.

In deterministic methods, the spatial domain of the problem is discretized into relatively fine spatial meshes to enable the approximation of spatial derivatives with finite differences. Thus, the spatial meshes must be small enough to allow this approximation (i.e., the particle density must not vary significantly within a mesh cell). Because the particle density varies with the material cross sections and the corresponding mean free path (mfp) (the average distance a particle travels between collisions), it is common practice to use mesh sizes of the order of 1 mfp to ensure that large variations do not occur and that the aforementioned approximation is valid.

Analogously, in Monte Carlo methods the particle statistical weight has been related to the adjoint function [Eq. (8)], which is also directly related to the material cross sections or mfp. Further, because the mfp is, by definition, the average distance a particle travels between collisions, it is a logical, problem-independent parameter by which particle statistical weight can be controlled. Therefore, during particle transport, the distance to collision is determined as before, but this distance is now compared to the mfp. If the distance to collision exceeds the user-defined mfp increment, the particle is transported the distance of that increment, and the statistical weight is compared to the weight window boundaries for that region. Parametric studies analyzing the effect of the increment of mfp on problem efficiency and reliability are deferred to Sec. IV.

The second issue of concern is the amount of time associated with checking the particle's statistical weight. The computational penalty in the Monte Carlo calculation for using larger numbers of spatial meshes or energy groups is related to the search routine. For the binary search (which is currently being used), the average number of comparisons in a successful search, assuming that each of the $N$ intervals is equally likely, is[40]

$$C_N = \log_2(N) + \frac{\log_2(N) + 2}{N} - 1 \ . \qquad (23)$$

The behavior is demonstrated in Table I. While in our problem each interval is not equally likely, the behavior is similar. Thus, the computational cost associated with increasing the number of intervals is a slowly increasing function (i.e., $\propto \log_2$) of the number of intervals.

TABLE I

Relationship Between Number of Intervals and Number of Comparisons

| Number of Intervals | Average Number of Comparisons |
|---|---|
| 2 | 1.50 |
| 10 | 2.85 |
| 50 | 4.79 |
| 100 | 5.73 |
| 1000 | 8.98 |

## IV. APPLICATION AND ANALYSIS

### *IV.A. One-Dimensional Test Problem*

For verification of implementation and performance testing, a simple one-dimensional test problem was developed. This problem is defined as a 150-cm slab of ordinary concrete with a fission source on the left-hand surface. The objective is to calculate the neutron tissue dose on the right-hand side of the slab.

To accelerate the Monte Carlo calculation, a one-dimensional adjoint distribution was calculated using the DORT code with the SAILOR $P_3$ 47-group library.[41] The deterministic model was constructed with 60 spatial meshes, each ~1 mfp or 2.5 cm thick. Figure 1 plots the adjoint distribution for a few representative energy groups and shows that the importance of each energy group varies by several orders of magnitude within the slab. Figure 1 also shows that while the slopes of the adjoints are similar for this problem, they vary significantly in magnitude.

For performance analysis, the test problem was run (a) without any variance reduction techniques beyond the default (in MCNP) implicit capture and (b) with the CADIS method in the modified version of MCNP for the purpose of variance reduction. Each case was allowed to run for 30 CPU-min on an IBM RISC/6000 model 370 computer.

If the Central Limit Theorem is valid, the estimated relative error squared $R^2$ should be proportional to $1/N$. Also, the computer time $T$ used in a Monte Carlo calculation should be directly proportional to $N$ (the number of histories); therefore, $R^2T$ should be approximately constant. Because in a Monte Carlo calculation it is desirable to minimize $R$ and $T$, the calculational efficiency is quantified in terms of the figure of merit[7] (FOM):

$$\mathrm{FOM} = \frac{1}{R^2T} \quad .$$

Therefore, the FOM will be used throughout this paper for comparisons of calculational efficiency.

The results of these calculations are listed in Table II and demonstrate that the CADIS method improves the efficiency of this calculation by a factor of ~2000 with

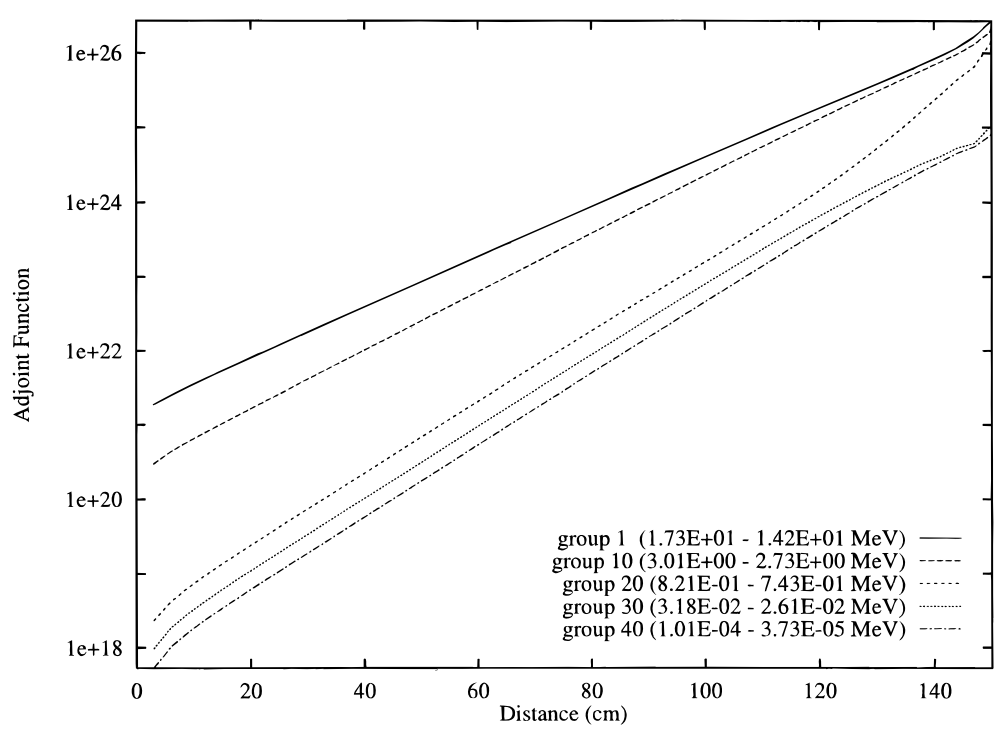


Fig. 1. Adjoint distributions in one-dimensional test problem.

TABLE II

Results of One-Dimensional Test Calculations

| Description | Number of Histories[a] | Dose (rem/h) | $R$[b] | VOV | FOM |
|---|---|---|---|---|---|
| MCNP | 2.8E+5[c] | 1.52E−12 | 0.874 | 0.9945 | 0.044 |
| MCNP with CADIS | 5.5E+4 | 1.36E−12 | 0.019 | 0.0023 | 91 |

[a]For 30 min of CPU time.
[b]$R \equiv$ relative error.
[c]Read as $2.8 \times 10^5$.

respect to the normal MCNP calculation. Practically, this means that the analog calculation would require ~43.7 CPU-days to reach the statistical precision of the CADIS results (obtained in 30 CPU-min).

As mentioned, parametric studies to analyze the effect of the increment of mfp on problem efficiency and reliability have been performed. The FOM is used as the measure of efficiency, while the figure of reliability[38] (FOR) is used as a measure of reliability and is calculated as follows:

$$\mathrm{FOR} = \frac{1}{(\mathrm{VOV})T} \quad ,$$

where VOV is the variance of the variance. Figure 2 shows the behavior of the FOM and FOR with varying increments of mfp for the one-dimensional test problem. In this simple one-dimensional example, both parameters follow expected behavior and peak at the same location. It is important to note that the peaks for both the FOM and FOR correspond to a mfp increment of 0.8, which is near unity.

### *IV.B. Reactor Cavity Dosimetry Calculation*

This problem addresses a major concern of nuclear utilities. The life of a reactor and its possible extension are directly limited by the embrittlement of the reactor pressure vessel (RPV), a low-carbon steel container surrounding the reactor core, under neutron irradiation. The embrittlement of the RPV material is primarily due to the bombardment of neutrons with energies greater than

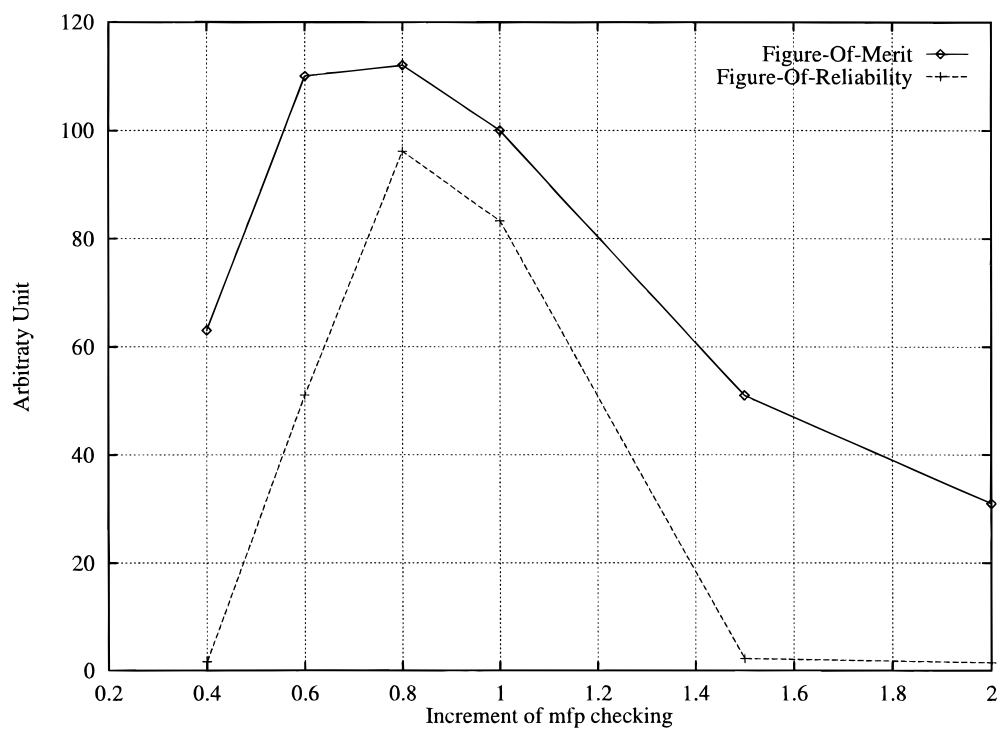


Fig. 2. Figure of merit and figure of reliability versus increment of mfp checking for one-dimensional test problem.

~1 MeV and cannot be directly determined from measured quantities. Radiation detectors are employed to provide data by which calculational methods/models can be validated. Often the dosimeter is outside the RPV, in what is referred to as the cavity; hence it is called cavity dosimetry. The cavity dosimetry calculations attempt to estimate high-energy (≥1.0/MeV) reaction rates in a small volume at a distance of ~350 cm from the core centerline and are used to validate methods/models that are subsequently used to estimate RPV integrity and provide a basis for plant life extension. The problem is illustrated in Fig. 3, which shows one octant of the Three Mile Island Unit 1 (TMI-1) reactor. In the past, the $S_N$ method was used, almost exclusively, to perform these calculations. More recently, the Monte Carlo method has been employed in an effort to better understand the uncertainties associated with the $S_N$ method and to attempt to validate $S_N$ calculations.[42–44]

Because of the computational expense, the Monte Carlo method is typically not used for such a large deep-penetration–type problem. Figure 4 shows the radial flux distributions from the core periphery to the cavity dosimeter for several energy groups and demonstrates that the flux decreases by ~5 orders of magnitude over this range. The error bars on this figure correspond to $1\sigma$ statistical uncertainties. As the neutrons travel outward in the radial direction from the core periphery (170 cm), they encounter the core barrel (179 to 184 cm), the thermal shield (187 to 192 cm), the RPV (217 to 239 cm), the cavity region (239 to 350 cm), and finally the cavity dosimeter (350 cm).

Without the use of variance reduction techniques, one could allow MCNP to run this problem continuously for weeks and still not obtain statistically significant/reliable results. In an effort to quantify the previous statement, this problem was modeled without the use of any variance reduction techniques, except for the energy cutoff, and allowed to run for an extensive amount of time. After simulating 100 million particle histories at a cost of ~50 h of CPU time, the ex-vessel cavity dosimeter tallies did not receive even a single particle score (i.e., not one of the 100 million particles made it to the ex-vessel cavity dosimeter). Based on the formulation for FOM, we may approximate the amount of computer time necessary to achieve a desired precision. From this, we find that it would require $\sim 1.2 \times 10^6$ min, or ~2.3 yr, of computer time to achieve a relative error of 5%. Hence, it is clear that variance reduction techniques are essential to achieving statistically meaningful results for an application of this type.

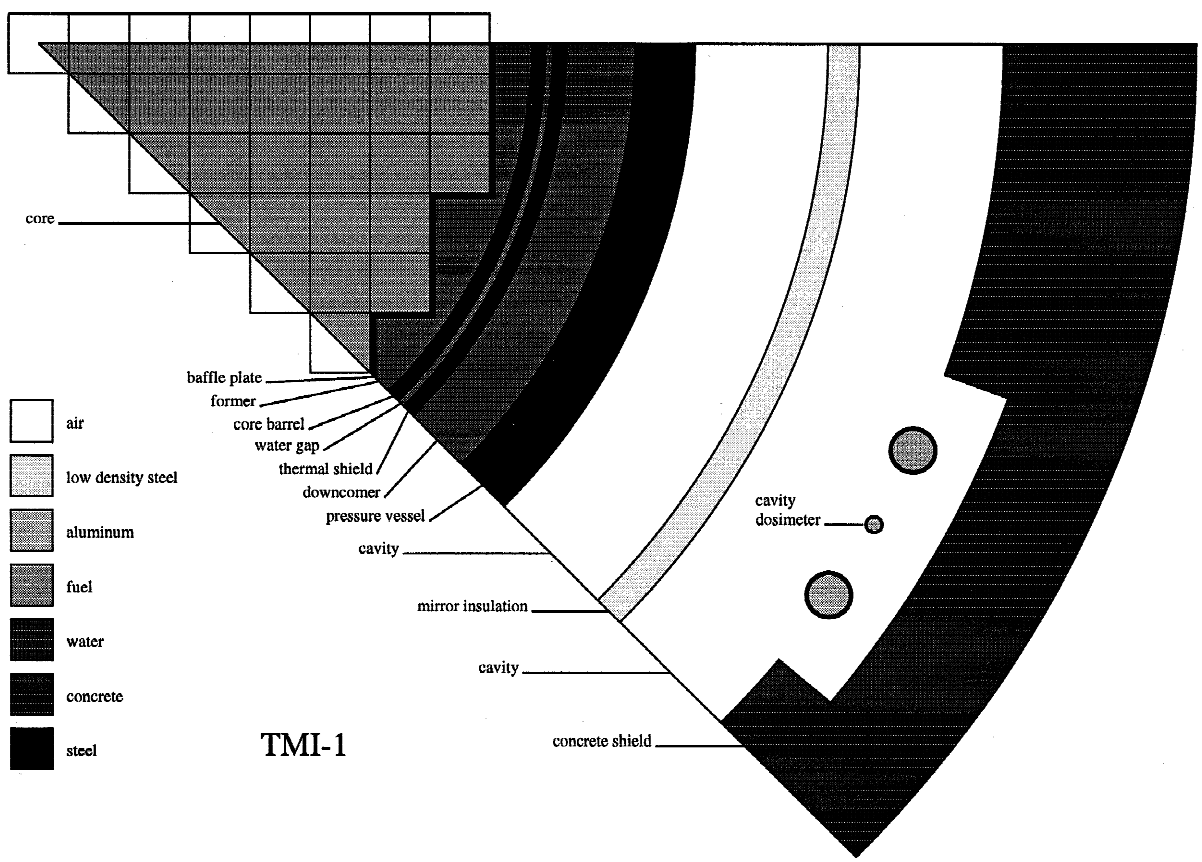


Fig. 3. One octant of the TMI-1 reactor.

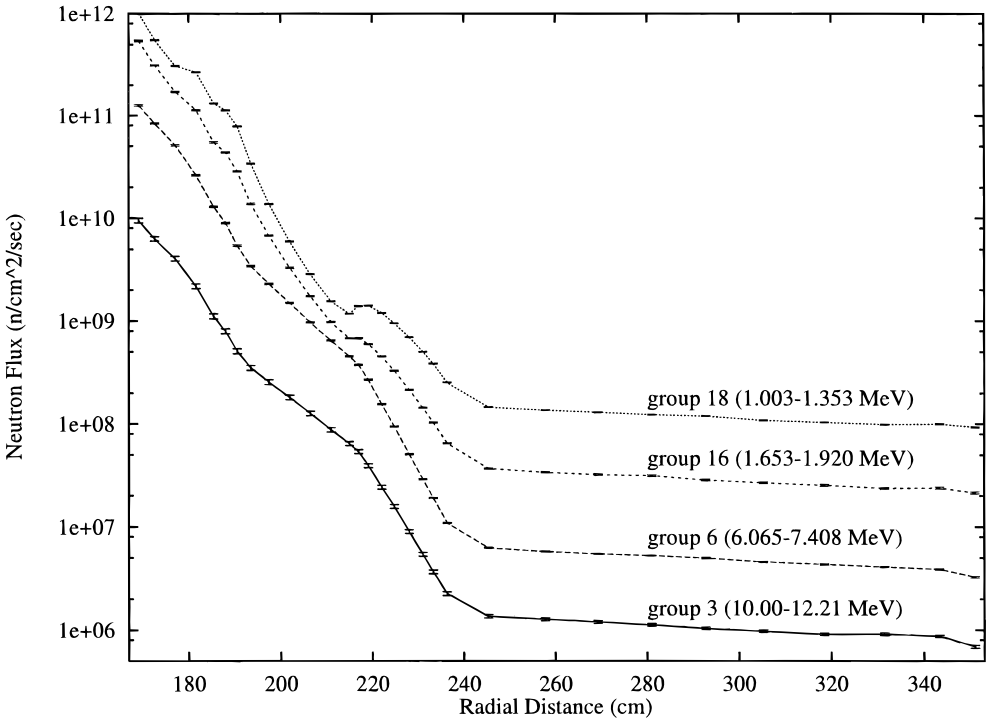


Fig. 4. Radial group flux distributions in the TMI-1 reactor.

### IV.B.1. Application of Existing Variance Reduction Methods

Before the CADIS method was developed and implemented into MCNP, the reactor cavity dosimetry calculation was manually optimized with existing variance reduction methods.[43] This manual optimization is now briefly described and will be used as a reference for evaluating the CADIS method.

MCNP (version 4A) offers several variance reduction techniques that are applicable to the cavity dosimetry calculation. The techniques chosen for this application include energy cutoff, source biasing, weight windows, and the exponential transformation. As the focus of the calculation is on high-energy neutrons that have experienced relatively few collisions, the energy cutoff was used to kill all particles with energies below 1 MeV, and the MCNP default implicit capture was turned off. Source biasing was used to start more particles with high energies and desirable directions, and the source from the inner assemblies was neglected.[43] Weight windows were used to describe the spatial- and energy-dependent importance of the particles and to control particle weight fluctuations, and finally, the exponential transformation technique was employed in the steel regions to stretch the distance between collisions in the direction of interest.

Initially, geometric splitting values based on intuition and a limited understanding of the physical system were used to perform some preliminary MCNP runs. The results of these runs created a better understanding of the cell importances and were subsequently used to refine the cell importances in an effort to maintain a relatively constant neutron density in the direction of the cavity dosimeter. After several iterations and modifications to the cell descriptions, a reasonable spatial importance function was obtained in the direction of the cavity dosimeter. The modifications to cell descriptions evolved from the desire to maintain reasonably small splitting ratios and thus consisted of decreasing the size of optically thick cells by dividing them into multiple cells of smaller radial thickness. The cell subdivision resulted in a factor of $\sim$12 increase in the number of cells in the problem description.

The geometric splitting parameters were then used as a starting point for the weight window generator to iteratively develop a spatial importance distribution for two energy groups. This process was extremely tedious and required a considerable amount of CPU time for the weight window generator runs, many iterations of significant smoothing and adjusting of the weight window values, and a great deal of physical understanding. The manual process of optimization was continued until the desired level of efficiency was achieved (i.e., additional efforts were no longer productive) with stable statistical behavior.

### IV.B.2. Application of CADIS

For this application, the $^{63}\mathrm{Cu}(n,\alpha)$, $^{58}\mathrm{Ni}(n,p)$, and $^{54}\mathrm{Fe}(n,p)$ reaction rates (responses), which have threshold

energies of ~5.0, ~1.0, and ~1.0 MeV, respectively, are all of equal interest, and thus we calculate an effective response function (shown in Fig. 5) as a normalized sum of each of the normalized response functions. Using this effective response function, we can generate an importance function that will simultaneously optimize the calculation for all three reaction rates and thus avoid calculating an importance function for each individual response that would require three separate Monte Carlo calculations.

With this effective response function as the adjoint source, a two-dimensional $R$-$\theta$ adjoint function is calculated with the DORT code[39] using the SAILOR 47-group library and a symmetric $S_8$ quadrature set. Figure 6 shows this adjoint function distribution for energy group 3 (10.00 to 12.14 MeV). The modified version of MCNP reads the adjoint function from the standard DORT binary flux file, couples the original source distributions with the adjoint function to generate the source-biasing parameters and weight window lower bounds, and then performs the transport calculation. The $S_N$ spatial mesh that is used within MCNP to define the spatial importance distribution is shown in Fig. 7. Within MCNP, the source spatial distribution is represented by a probability distribution function at 24 axial locations in each fuel pin of the last two (peripheral) layers of assemblies, and the energy distribution is based on an equivalent fission spectrum for the uranium and plutonium fissile isotopes.[45] The following approximations/assumptions are made in this process: (a) The axial behavior for the adjoint function is approximated with a cosine distribution, and (b) to represent the spatial dependence of the energy-biasing parameters, the energy-dependent adjoint function is averaged over each user-defined spatial source cell, and a dependent source-energy–biasing distribution is calculated for each source cell. For this particular application, each assembly has an associated source-energy–biasing distribution. No modifications to the source routines are necessary because the capabilities to handle source variable biasing and dependent source distributions are standard features of the MCNP code.

Because the focus of this work is on the automatic variance reduction for the calculation and not on the calculation itself, the interested reader is referred to Refs. 42 and 43 for discussions regarding the accuracy of results with respect to measurements and $S_N$ calculations, as well as sensitivity studies related to various aspects of this calculation. However, to provide some idea about the accuracy and to demonstrate that the automatic variance reduction technique does not bias the calculation, calculated-to-experimental (C/E) ratios, corresponding to ENDF/B-V material and SAILOR dosimetry cross sections, are given in Table III. The differences between C/E ratios calculated with the manually optimized model and with the automatic variance reduction method are consistent with the statistical uncertainties.

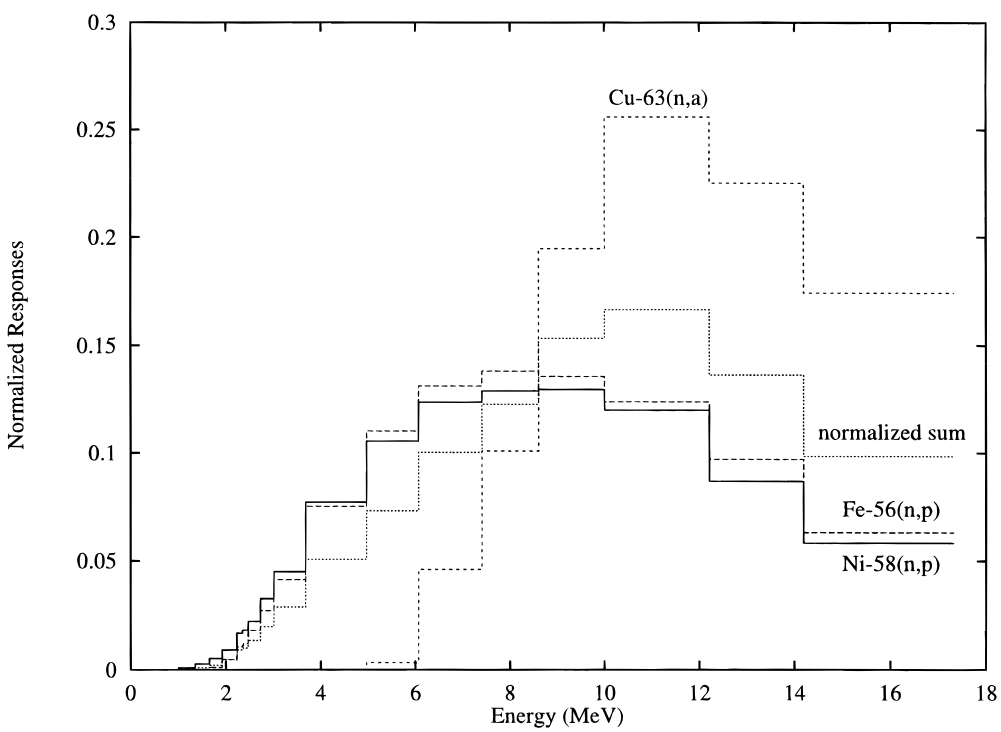


Fig. 5. Response functions.

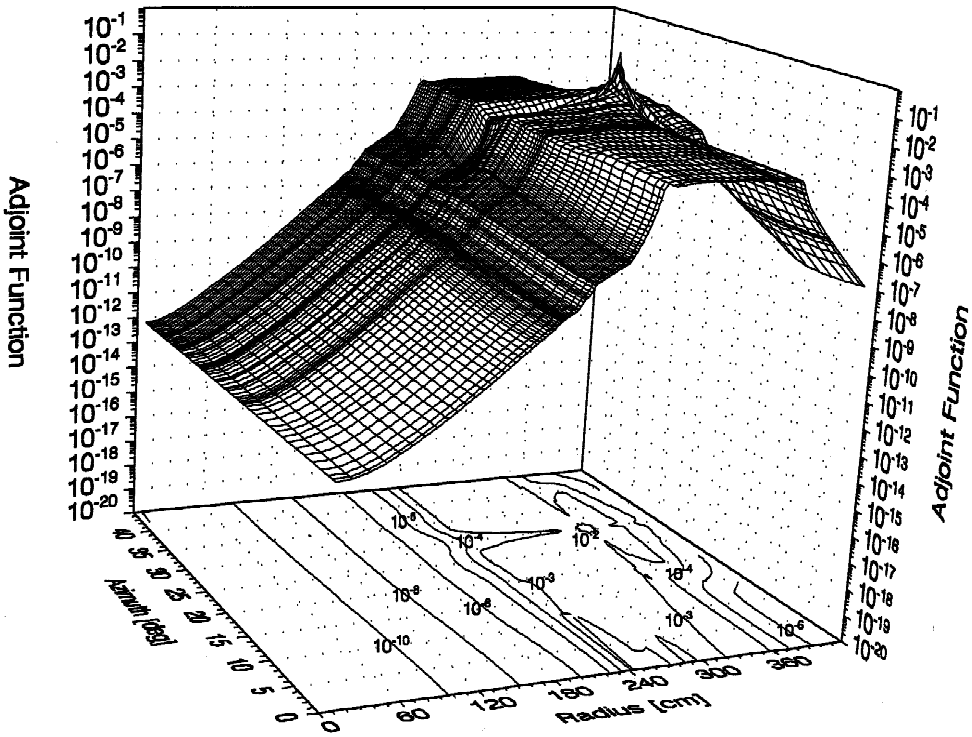


Fig. 6. Adjoint function distribution for energy group 3 (10.00 to 12.14 MeV).

IV.B.3. Comparison of Calculational Efficiency

With the use of the automatic variance reduction method, the computer time required by the MCNP model to calculate the reaction rates at the ex-vessel cavity dosimeter with $1\sigma$ uncertainties of $<3\%$ is $\sim 1$ h on an IBM RISC/6000 model 370. To reach the same precision (3%) with the manually optimized model requires nearly 5 h of CPU time. This behavior is demonstrated in Fig. 8, which plots relative error ($R$) versus computer time for the three reaction rates of interest. Also included in Fig. 8 is a curve representing the ideal behavior, $R \propto 1/\sqrt{T}$. The two sets of curves in Fig. 8 correspond to calculations performed with different variance reduction approaches, namely manually optimized variance reduction [including energy cutoff, source biasing, weight windows (2 energy groups), and the exponential transformation; see Ref. 43 for details] and the automatic variance reduction derived from a two-dimensional adjoint function distribution (18 energy groups) using the effective response function.

Table III lists the FOM values [FOM $= 1/(R)^2T$] and reveals that the use of the automatic variance reduction increases the calculational efficiency by a factor of $>4$ with respect to our best manually optimized model (note that the observed increase in efficiency is dependent upon the quality and detail of the manual optimization). Further, the use of the automatic variance reduction can be shown to increase the calculational efficiency by a factor of $\sim 10^4$ with respect to the analog case.

In an effort to evaluate the use of the effective response function, automatic variance reduction calculations were also performed for each individual response function separately (i.e., an adjoint calculation was performed with each response function and used in individual MCNP calculations). Table IV lists the FOM values for these calculations. The use of individual adjoint functions is shown to increase the efficiency by a factor of $\sim 7$ with respect to the single manually optimized importance function and by $\sim 35\%$ with respect to the adjoint function with an effective response function. The use of the individual response functions required two more DORT and MCNP calculations than the use of a single effective response function. Considering the CPU time for these additional calculations, the use of an effective response function is actually more efficient for this problem.

It should be noted that the aforementioned CPU times do not include the $S_N$ adjoint calculation. Also, for the purpose of comparison, the synthesized three-dimensional deterministic results (group fluxes for energies greater than $\sim 1$ MeV) can be produced by two two-dimensional and one one-dimensional calculations that require $\sim 0.25$, 0.25, and 0.005 h of CPU time, respectively, on an IBM RISC/6000 model 370. The CPU time required for the synthesis process is essentially negligible. Thus, group

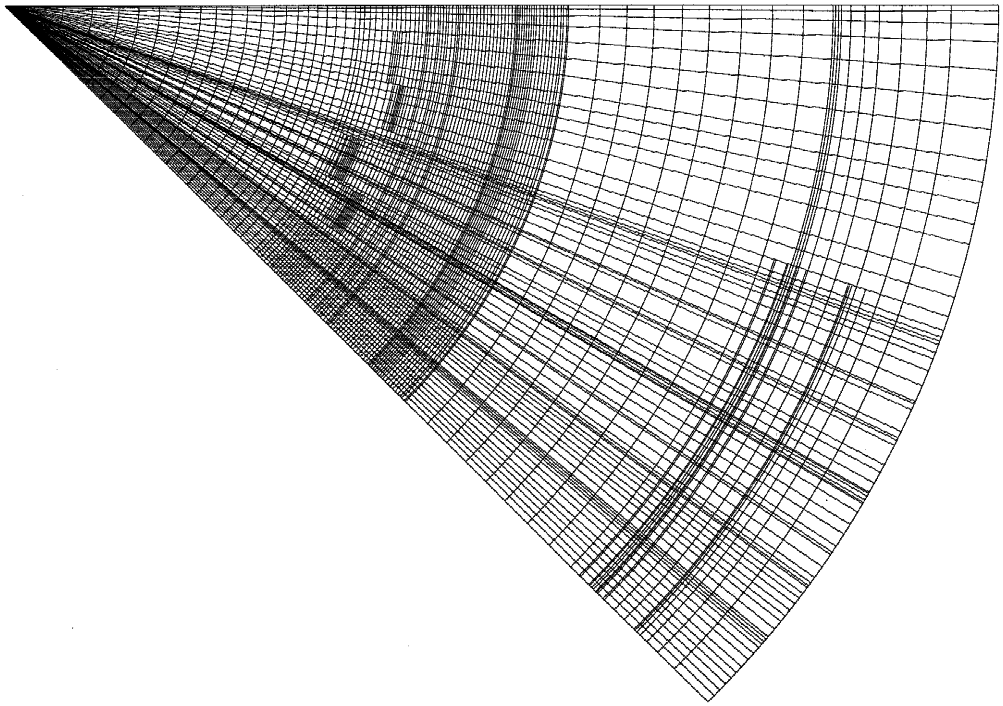

Fig. 7. $S_N$ spatial mesh used to facilitate the spatial importance distribution.

fluxes over the entire spatial domain can be generated by DORT in <1 CPU-h.

Figure 9 shows the behavior of the FOM with varying increments of mfp for the three-dimensional reactor cavity dosimetry calculation using the $^{58}$Ni$(n,p)$ response function and demonstrates the appropriateness and problem independence of using a value near unity for the increment of mfp parameter.

To provide an indication of the computational penalty associated with weight checking, the percentage of total time spent processing the weight windows and total computational time spent in the spatial searching routine as a function of the increment of mfp are plotted in Fig. 10. This figure demonstrates that for an increment of mfp near unity, ~24% of the total computational time is spent processing the weight windows, and ~10% of the total time is spent in the spatial portion of the weight checking alone. This result has motivated attempts to develop more clever search routines. However, no significant gains have been achieved. Based on the results shown in Figs. 2, 9, and 10, the default value for the increment of mfp is unity.

TABLE III

Calculated-to-Experimental Ratios at the Cavity Dosimeter for TMI-1

| Reaction | Manually Optimized | | Automatic Variance Reduction | |
|---|---|---|---|---|
| | C/E | FOM | C/E | FOM |
| $^{63}$Cu$(n,\alpha)$ | 0.905(0.022)[a] | 3.7 | 0.878(0.022) | 16 (4.3)[b] |
| $^{54}$Fe$(n,p)$ | 0.965(0.023) | 3.5 | 0.964(0.020) | 20 (5.7) |
| $^{58}$Ni$(n,p)$ | 0.947(0.020) | 4.5 | 0.952(0.019) | 22 (4.9) |

[a]$1\sigma$ uncertainties.

[b]Ratio of "Automatic Variance Reduction" and "Manually Optimized" FOMs.

### IV.B.4. Comparison of Calculational Reliability

One potential problem associated with the intense use of variance reduction techniques is erratic or unreliable error estimations. Figure 8 shows that the relative error follows the expected behavior predicted by the Central Limit Theorem ($R \sim 1/\sqrt{N} \sim 1/\sqrt{T}$, where $N$ is the number of particle histories), which provides some indication about the validity of the estimated relative errors. The use of the automatic variance reduction method appears to lead to smoother statistical convergence. All three reaction rate tallies pass all ten of the MCNP statistical checks,[7] providing an additional indication of proper statistical convergence.

To further assess the estimated uncertainties, the manually optimized and automatic variance reduction cases were each run ten times with different starting random

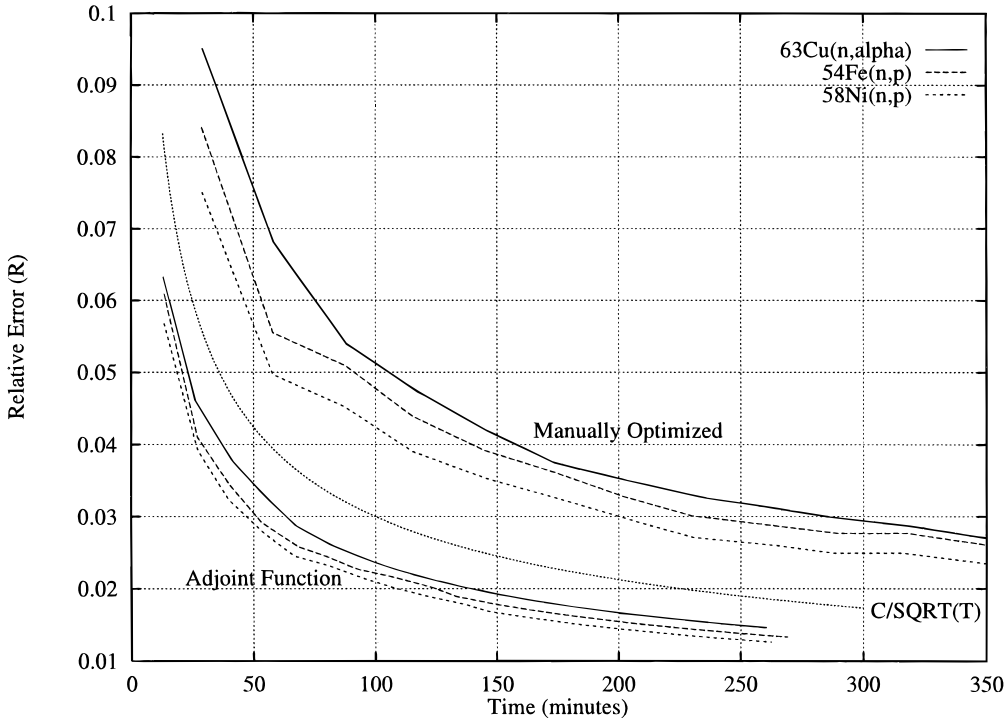


Fig. 8. Relative error versus computer time.

number seeds. This allows us to compare the relative error as estimated by MCNP to the relative standard deviation of the calculated means (reaction rates) from the multiple runs. The number of histories was chosen such that both cases would yield similar $R$'s; the manually optimized and automatic variance reduction cases required $20 \times 10^6$ and $3 \times 10^6$ particle histories, respectively. Table V compares the calculated relative standard deviations to the average (MCNP) estimated relative errors and reveals that the relative error is underestimated by as much as 20% in the manually optimized case and overestimated by >20% in the automatic variance reduction case. In other words, the estimated relative errors from the automatic variance reduction case are more conservative than those from the manually optimized case.

For a normal distribution, the calculated value should be within the $1\sigma$ relative error 68% of the time. For our ten runs (with three reaction rates per run), the calculated values are observed to be within the $1\sigma$ relative error 57% of the time for the manually optimized case and 87% of the time for the automatic variance reduction case. In addition, the standard deviation of the estimated relative errors and the estimated VOV's are a factor of ~3 less in the automatic variance reduction case than in the manually optimized case. These results clearly demonstrate that the automatic variance reduction method produces reliable/conservative error estimations.

TABLE IV

Effect of Response Functions on FOMs at the Cavity Dosimeter for TMI-1

| Reaction | Effective Response Function | | Individual Response Function | |
|---|---|---|---|---|
| | C/E | FOM | C/E | FOM |
| $^{63}$Cu$(n,\alpha)$ | 0.878(0.022)[a] | 16 (4.3)[b] | 0.882(0.019)[a] | 25 (6.8)[b] |
| $^{54}$Fe$(n,p)$ | 0.964(0.020) | 20 (5.7) | 0.953(0.016) | 28 (8.0) |
| $^{58}$Ni$(n,p)$ | 0.952(0.019) | 22 (4.9) | 0.923(0.015) | 30 (6.7) |

[a] $1\sigma$ uncertainties.

[b] Ratio of "Automatic Variance Reduction" and "Manually Optimized" FOMs.

## V. EFFECT OF ADJOINT ACCURACY

The effectiveness of an adjoint (importance) function for variance reduction of Monte Carlo calculations is dictated by its accuracy. It is for this reason that we use an accurate method—the $S_N$ method—to calculate the adjoint function. However, for extremely large problems and for the extension to three-dimensional adjoint functions, the memory and disk space requirements for the $S_N$ adjoint calculations can become prohibitive. One way to alleviate this problem is to sacrifice some of the

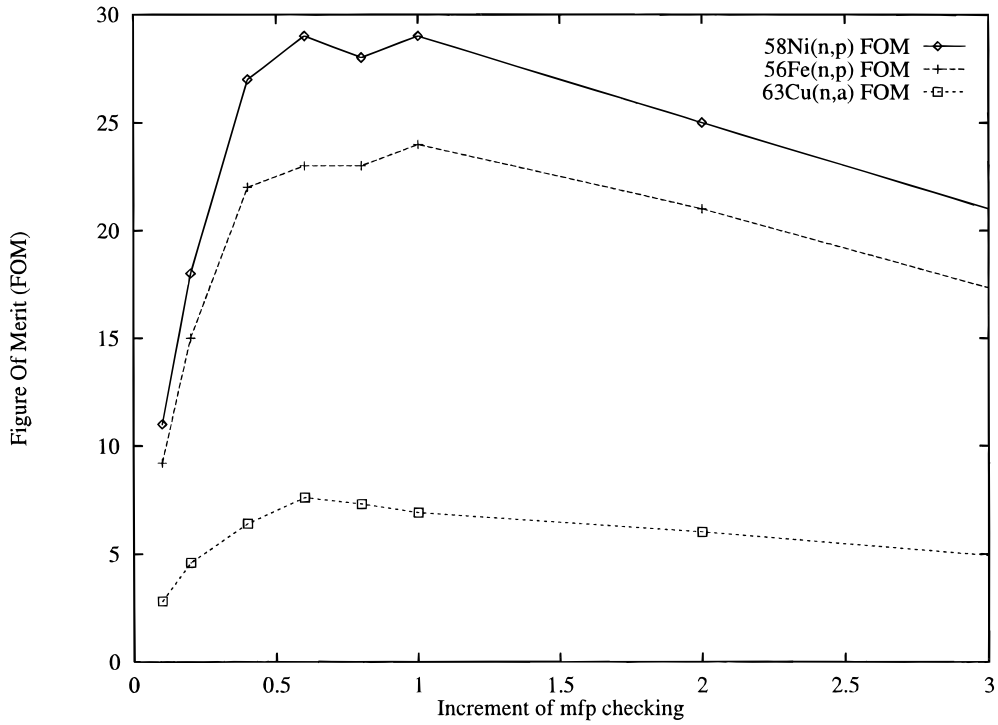


Fig. 9. Figure of merit versus increment of mfp checking for the reactor cavity calculation.

accuracy of the adjoint calculation through the use of fewer energy groups. However, the relationship between the accuracy of adjoint functions and their effectiveness for variance reduction of Monte Carlo calculations is problem dependent and is not well known. Therefore, in this section we investigate the effectiveness of importance functions with varying degrees of energy- and spatial-dependent accuracy.

### *V.A. Energy Dependence*

To examine the effect of using an adjoint function with varying numbers of energy groups, one of the following two approaches may be employed: (a) collapse an appropriate multigroup library into various libraries with fewer groups and use these libraries to calculate adjoint functions or (b) calculate the adjoint function for a given number of (maximum) groups and collapse it into various coarse-group structures. In this study, we have chosen the second approach because it does not require the generation of additional multigroup libraries and subsequent $S_N$ calculations, and it uses an accurate importance function as its starting point. In other words, this method eliminates concerns related to the selection of multigroup boundaries for the cross-section collapsing procedure; specifically, the effect of their selection on the accuracy of the $S_N$ solution.

To collapse an adjoint function into fewer groups, it is necessary to introduce group quantities such that the total response $R$,

$$R = \int_V \int_E \phi^\dagger(r,E) q(r,E)\, dE\, dV \ , \tag{24}$$

is conserved. This is done by setting the integral equal to the product of the adjoint function and the source in coarse group $g$:

$$\int_g \phi^\dagger(r,E) q(r,E)\, dE = \phi_g^\dagger(r) q_g(r) \ , \tag{25}$$

where we define the coarse-group source and adjoint by

$$q_g = \int_g q(r,E)\, dE$$

and

$$\phi_g^\dagger = \frac{\int_g \phi^\dagger(r,E) q(r,E)\, dE}{q_g} \ . \tag{26}$$

This procedure formally preserves the total response and leads to the definition of a coarse-group adjoint through source weighting. Because of the source weighting, these relations are only applicable within the source region.

However, for this study, it is necessary to collapse the adjoint throughout the problem; i.e., including regions

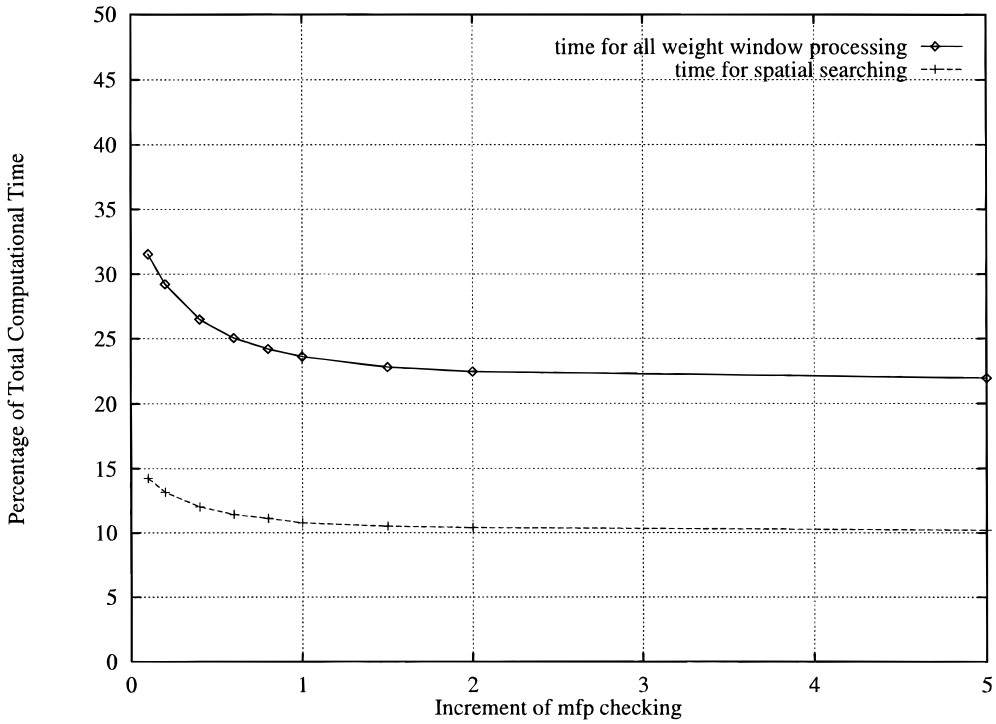


Fig. 10. Searching time versus increment of mfp checking for the reactor cavity calculation.

outside the source region(s). To do this, it is necessary to conserve the response from each spatial region. Because the forward flux in a spatial region can be considered to be the source of particles within that region, it may be used to weight the adjoint in the collapsing procedure. Replacing the source term with the forward flux in the preceding relations yields

$$\int_g \phi^\dagger(r,E)\phi(r,E)\,dE = \phi_g^\dagger(r)\phi_g(r) \ , \tag{27}$$

where we define the coarse-group flux and adjoint by

$$\phi_g = \int_g \phi(r,E)\,dE$$

and

$$\phi_g^\dagger = \frac{\int_g \phi^\dagger(r,E)\phi(r,E)\,dE}{\phi_g} \ . \tag{28}$$

A computer program was written to read the DORT binary flux files from forward and adjoint calculations, perform the collapse as just discussed, and generate a collapsed adjoint binary flux file in the same format. This allows the current modified version of MCNP to read and utilize the various collapsed adjoint functions without additional modifications.

TABLE V

Comparison of Estimated Relative Errors and Calculated Relative Standard Deviations at the Cavity Dosimeter

| Reaction | Manually Optimized | | | Automatic Variance Reduction | | |
|---|---|---|---|---|---|---|
| | Average Estimated $R$[a] | Calculated Relative Standard Deviation[b] | Ratio | Average Estimated $R$[a] | Calculated Relative Standard Deviation[b] | Ratio |
| $^{63}$Cu$(n,\alpha)$ | 0.0229 | 0.0198 | 0.86 | 0.0223 | 0.0178 | 0.799 |
| $^{54}$Fe$(n,p)$ | 0.0203 | 0.0243 | 1.20 | 0.0197 | 0.0132 | 0.668 |
| $^{58}$Ni$(n,p)$ | 0.0181 | 0.0200 | 1.10 | 0.0189 | 0.0142 | 0.750 |

[a]Refers to the average of the relative errors estimated by MCNP in the ten runs.
[b]Refers to the relative standard deviation of the calculated reaction rates in the ten runs.

### V.A.1. One-Dimensional Test Problem

To evaluate this collapsing procedure and subsequently the effectiveness of a coarse-group adjoint function for variance reduction of the aforementioned one-dimensional concrete slab problem, the original 47-group adjoint is collapsed into 24-, 12-, 5-, 2-, and 1-group adjoint functions. The coarse-group boundaries are a subset of the fine-group boundaries, and each coarse group contains the same number of fine groups (except for the last group because the ratio of the number of fine groups and the number of coarse groups is not an integer). For example, in the 12-group structure, the highest energy group contains the highest four groups of the 47-group structure.

With these collapsed adjoint functions, MCNP calculates source-biasing parameters and weight window lower bounds. The effect of the collapse on the source-biasing parameters is illustrated in Figs. 11 and 12.

Figure 13 shows the relationship between the number of adjoint energy groups and the Monte Carlo calculational efficiency in terms of FOM. The FOM values are normalized such that the highest value is unity. The figure demonstrates that for this calculation there is some benefit to using 47 groups as opposed to 24 groups. However, the benefit is very small (~5%), and the increase in time required by the $S_N$ calculation with twice the number of energy groups is not represented. In general, Fig. 13 shows diminishing increases in efficiency with larger numbers of energy groups (beyond ~20 groups). For example, while the maximum increase in efficiency with respect to the unbiased case is ~2000, the increase in efficiency associated with using a collapsed 2-group adjoint is ~850. Thus, for this particular problem, an adjoint with few energy groups (~2 to 5 groups) is capable of increasing the calculational efficiency by approximately half as much as the adjoint with 47 groups.

### V.A.2. Reactor Cavity Dosimetry Calculation

For analysis wth this problem, the 18-group (energy groups above 1 MeV) adjoint is collapsed into 9-, 6-, 3-, 2-, and 1-group adjoint functions.

Figure 14 shows the relationship between the number of adjoint energy groups and the Monte Carlo calculational efficiency in terms of FOM. The FOM values are normalized such that the highest value is unity. The figure demonstrates that for the $^{54}Fe(n,p)$ and $^{58}Ni(n,p)$ reaction rate calculations there is no benefit to using more than ~9 groups, and relatively minor losses in efficiency are associated with using fewer energy groups (i.e., 2 to 6 groups). On the other hand, because the $^{63}Cu(n,\alpha)$ reaction rate calculation is sensitive to a rather narrow

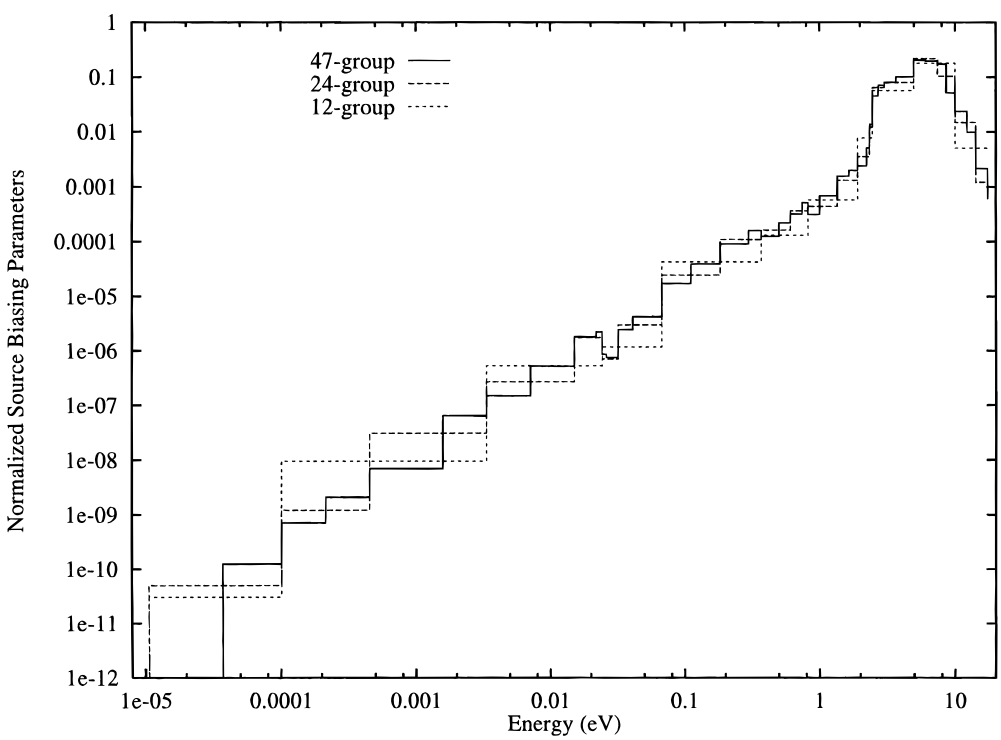


Fig. 11. Comparison of fine- and coarse-group source-biasing parameters.

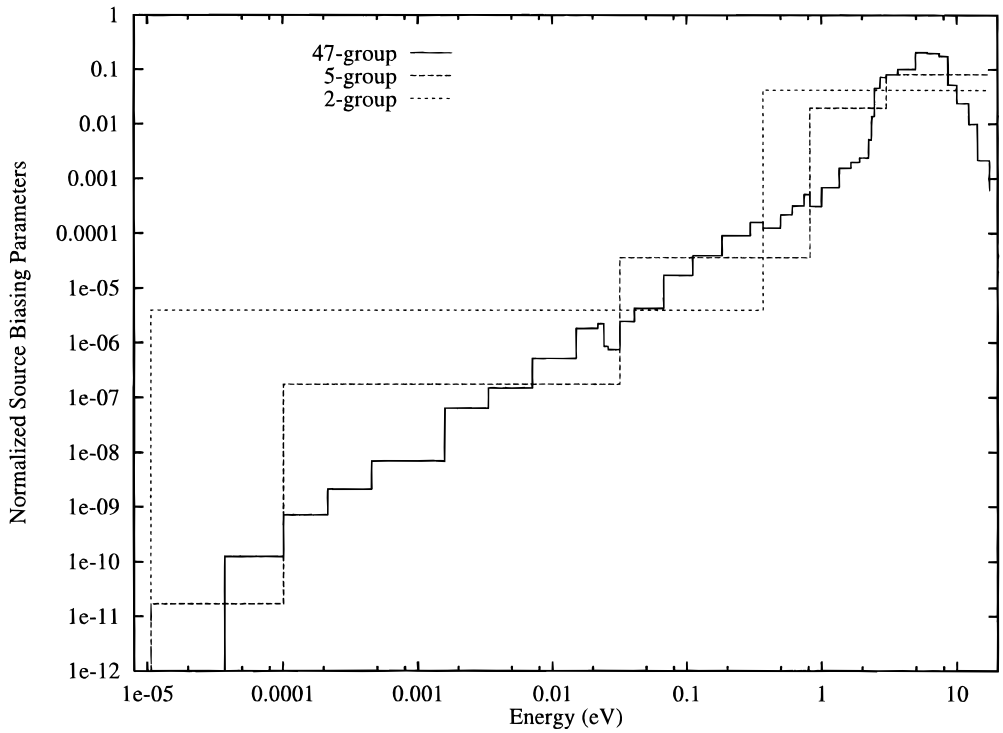


Fig. 12. Comparison of fine- and coarse-group source-biasing parameters.

energy range (~6 to 12 MeV), larger losses in efficiency are observed when fewer energy groups are used. Nevertheless, for this particular problem, an adjoint with few energy groups (~3 groups) is capable of increasing the calculational efficiency to approximately half of the observed maximum, which is a factor of $\sim 10^4$ more efficient than the analog case.

### *V.B. Spatial Dependence*

For solution using the $S_N$ method, as well as other deterministic methods, the spatial domain is discretized into spatial meshes to enable the approximation of spatial derivatives with finite differences. Naturally, the accuracy of this approximation is dependent on the size of the spatial meshes. To examine the effect of the $S_N$ adjoint mesh size on effectiveness for Monte Carlo variance reduction, $S_N$ adjoint calculations with mesh sizes ranging from 0.5 to 4 mfp's were performed. These adjoints were then used to accelerate Monte Carlo calculations for the one-dimensional test problem. The effect of the adjoint mesh size on Monte Carlo calculational efficiency in terms of FOM is shown in Fig. 15. The FOM associated with mesh sizes as large as 4 mfp's is shown to be ~50% of the maximum observed value (corresponding to 0.5 mfp). Thus, the dependence of the FOM on mesh size is relatively minor for this problem.

## VI. SUMMARY

A general method for automatically calculating and using variance reduction parameters for Monte Carlo shielding calculations based on the space- and energy-dependent $S_N$ adjoint function has been developed and presented. The theory supporting the use of the adjoint function for variance reduction of Monte Carlo calculations is based on the physical interpretation of the adjoint function. The equations for determining the source-biasing and weight window parameters were consistently derived from basic importance sampling with the adjoint function as the weighting function, and thus, the method is referred to as CADIS, Consistent Adjoint Driven Importance Sampling.

The CADIS method eliminates the manual process of selecting variance reduction parameters and thus can significantly reduce the amount of experience, time, and effort required for preparing and performing large Monte Carlo calculations. In addition, because the deterministic adjoint function is a far more accurate importance function than even an experienced variance reduction user is capable of creating, it is more efficient and reliable for variance reduction of Monte Carlo calculations.

This method is implemented into the general-purpose Monte Carlo code MCNP. Currently, this modified version of MCNP is able to (a) read the adjoint function and

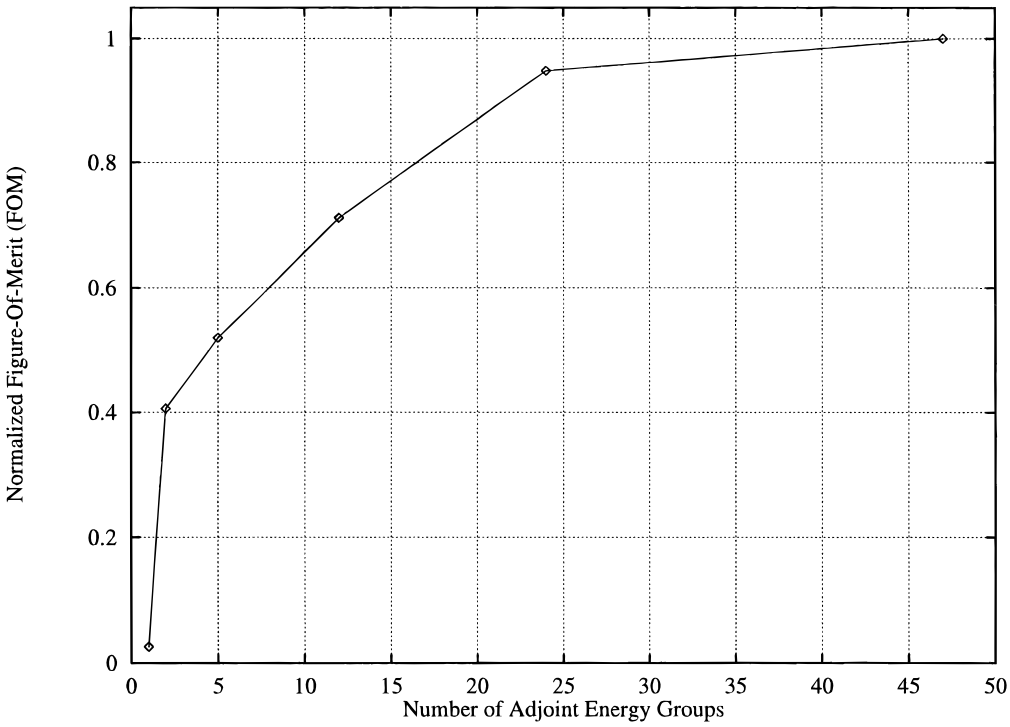


Fig. 13. Effect of number of adjoint energy groups on FOM.

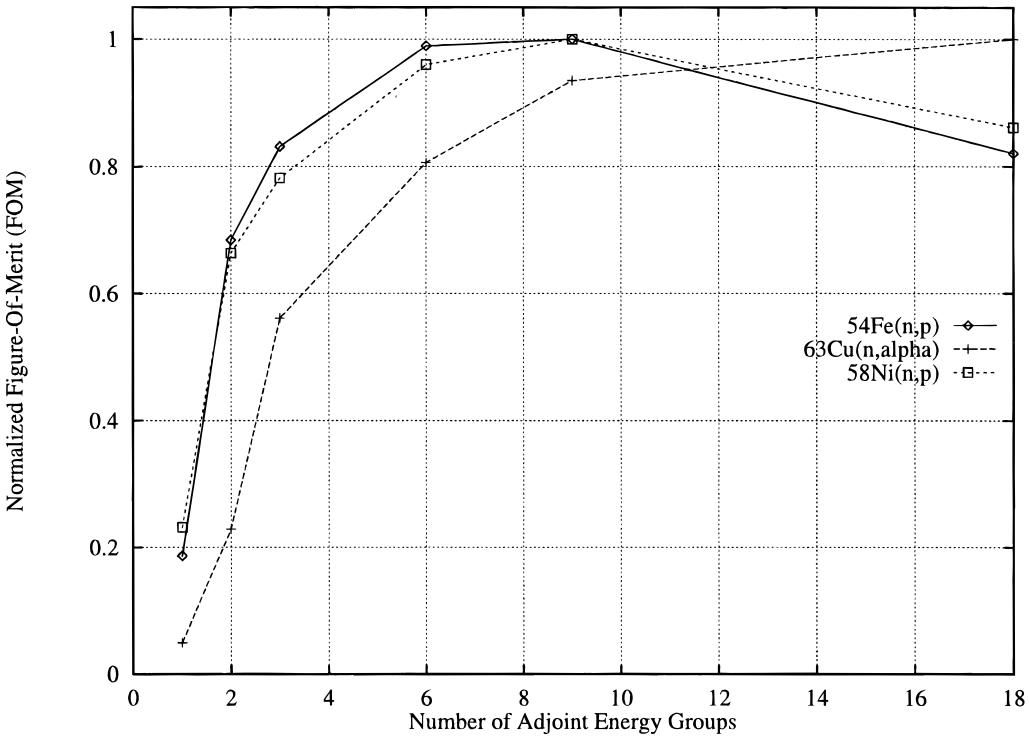


Fig. 14. Effect of number of adjoint energy groups on FOM.

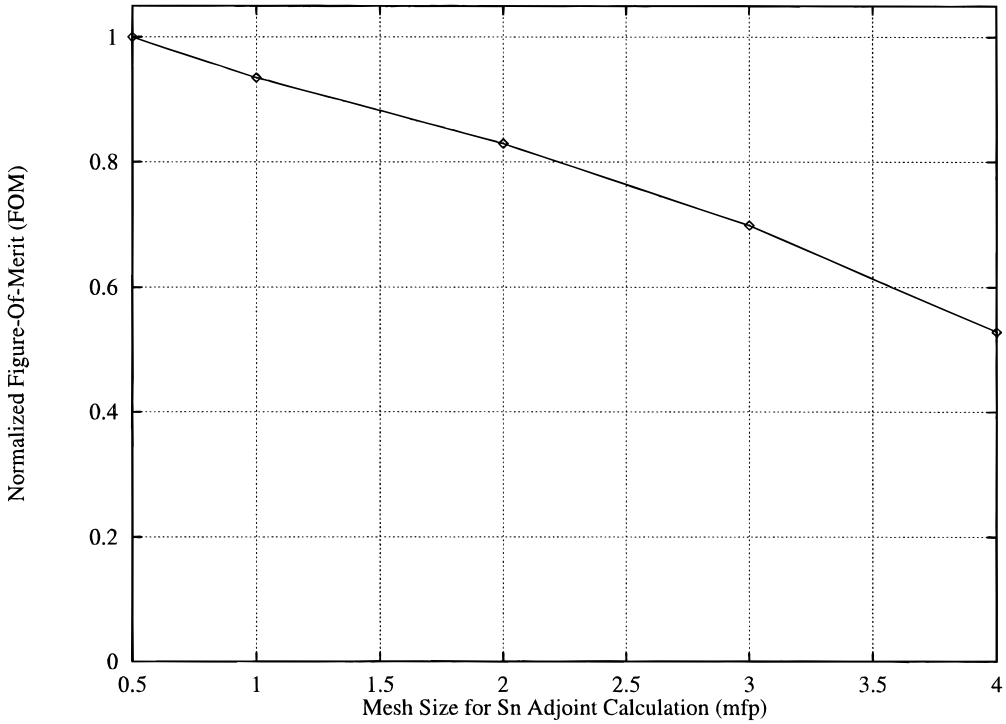


Fig. 15. Effect of adjoint mesh size on FOM.

the variable spatial mesh and energy-group information from a standard $S_N$ code (DORT) binary flux file, (b) superimpose the variable spatial mesh and energy grid onto the MCNP problem, (c) couple the original source distributions with the adjoint function to generate dependent source-biasing parameters and weight window lower bounds, and (d) perform the transport calculation using the constructed grids and calculated parameters. Various concepts for minimizing the amount of computational overhead associated with this process, such as when to check the weight and what searching schemes to use, have been examined.

The effectiveness of this method within the modified version of MCNP has been verified through its application to a realistic shielding calculation, namely the reactor cavity dosimetry calculation. With the use of the automatic variance reduction method, the efficiency of the reaction rate calculation was shown to increase by a factor of $>4$, and the statistical convergence was improved with respect to our best manually optimized model. Perhaps as important as its ability to increase the calculational efficiency is the fact that it does so in a way that requires very little time or experience on the part of the user. Because it is based on the source-biasing and weight window techniques, the method is practical and features statistical reliability and general applicability. In addition, the method does not in any way restrict the accuracy of the explicit three-dimensional continuous energy and angular Monte Carlo method.

## VII. RECENT DEVELOPMENTS

The limitation of this type of approach is the requirement for an $S_N$ adjoint solution, which requires the user to be knowledgeable in both Monte Carlo and deterministic methods, which is not often the case. To overcome this difficulty, algorithms have been developed and implemented into MCNP for automatically generating input files for $S_N$ adjoint calculations directly from the MCNP input, including mesh generation and material cross-section preparation. This automation eliminates the tedious process of manually generating these files and requires very little experience on the part of the user with regard to $S_N$ adjoint calculations.

The coupling to MCNP of these modifications, (a) the automatic generation of input files for $S_N$ adjoint calculations and (b) the automatic calculation and utilization of variance reduction parameters from $S_N$ adjoint functions, has resulted in the complete automation of variance reduction for MCNP shielding calculations. This will be the subject of future papers.

## ACKNOWLEDGMENTS

The authors would like to acknowledge the equipment grant of two IBM RISC/6000 workstations from the IBM Corporation and the computer resources provided by the Penn State Center for Academic Computing. The authors would also like to thank B. G. Petrovic for valuable discussions and the original DORT model of TMI-1.

## REFERENCES


1. R. A. FORSTER, S. P. PEDERSON, and T. E. BOOTH, "Ten New Checks to Assess the Statistical Quality of Monte Carlo Solutions in MCNP," *Proc. 8th Int. Conf. Radiation Shielding*, Arlington, Texas, April 24–28, 1994, Vol. 1, p. 414, American Nuclear Society (1994).

2. I. LUX and L. KOBLINGER, *Monte Carlo Particle Transport Methods: Neutron and Photon Calculations*, CRC Press, Boca Raton, Florida (1990).

3. M. H. KALOS et al., "Monte Carlo Methods in Reactor Computations," *Computing Methods in Reactor Physics*, H. GREENSPAN et al., Eds., Gordon and Breach Publishers, New York (1968).

4. M. H. KALOS and P. A. WHITLOCK, *Monte Carlo Methods—Volume 1: Basics*, John Wiley & Sons, New York (1986).

5. L. L. CARTER and E. D. CASHWELL, *Particle Transport Simulation with the Monte Carlo Method*, ERDA Critical Review Series, TID-26607 (1975).

6. S. N. CRAMER and J. S. TANG, "Variance Reduction Methods Applied to Deep-Penetration Monte Carlo Problems," ORNL/TM-9643, Oak Ridge National Laboratory (1986).

7. "MCNP—A General Monte Carlo N-Particle Transport Code, Version 4A," LA-12625, J. F. BRIESMEISTER, Ed., Los Alamos National Laboratory (1993).

8. M. B. EMMETT, "The MORSE Monte Carlo Radiation Transport Code System," ORNL-4972, Oak Ridge National Laboratory (1975).

9. S. CHUCAS, I. CURL, T. SHUTTLEWORTH, and G. MORRELL, "Preparing the Monte Carlo Code MCBEND for the 21st Century," *Proc. 8th Int. Conf. Radiation Shielding*, Arlington, Texas, April 24–28, 1994, Vol. 1, p. 381, American Nuclear Society (1994).

10. J. P. BOTH, H. DERRIENNIC, B. MORILLON, and J. C. NIMAL, "A Survey of TRIPOLI-4," *Proc. 8th Int. Conf. Radiation Shielding*, Arlington, Texas, April 24–28, 1994, Vol. 1, p. 373, American Nuclear Society (1994).

11. T. E. BOOTH and J. S. HENDRICKS, "Importance Estimation in Forward Monte Carlo Calculations," *Nucl. Technol./Fusion*, **5**, 90 (1984).

12. J. L. MacDONALD, "Investigation of Pattern Recognition Techniques for the Identification of Splitting Surfaces in Monte Carlo Particle Transport Calculations," LA-6015-T, Los Alamos National Laboratory (1975).

13. O. L. DEUTSCH and L. L. CARTER, "Simultaneous Global Calculation of Flux and Importance with Forward Monte Carlo," *Proc. 5th Int. Conf. Reactor Shielding*, Knoxville, Tennessee, April 18–22, 1977, p. 580, Science Press (1977).

14. M. GOLDSTEIN and E. GREENSPAN, "A Recursive Monte Carlo Method for Estimating Importance Function Distributions in Deep-Penetration Problems," *Nucl. Sci. Eng.*, **76**, 308 (1980).

15. T. E. BOOTH, "Automatic Importance Estimation in Forward Monte Carlo Calculations," *Trans. Am. Nucl. Soc.*, **41**, 308 (1982).

16. T. E. BOOTH, "A Weight Window/Importance Generator for Monte Carlo Streaming Problems," *Proc. 6th Int. Conf. Radiation Shielding*, Tokyo, Japan, May 16–20, 1983, Vol. I, p. 210, Japan Atomic Energy Research Institute (1983).

17. A. DUBI, T. ELPERIN, and D. J. DUDZIAK, "Geometrical Splitting in Monte Carlo," *Nucl. Sci. Eng.*, **80**, 139 (1982).

18. A. DUBI, N. GUGVITZ, and K. BURN, "Optimal Space-Energy Splitting in MCNP with the DSA," *Prog. Nucl. Energy*, **24**, 11 (1990).

19. K. W. BURN, "Optimizing Cell Importances Using an Extension of the DSA—Theory Implementation, Preliminary Results," *Prog. Nucl. Energy*, **24**, 39 (1990).

20. K. W. BURN, "Extending the Direct Statistical Approach to Include Particle Bifurcation Between the Splitting Surfaces," *Nucl. Sci. Eng.*, **119**, 44 (1995).

21. T. E. BOOTH, "A Sample Problem in Variance Reduction in MCNP," LA-10363-MS, Los Alamos National Laboratory (1985).

22. G. I. BELL and S. GLASSTONE, *Nuclear Reactor Theory*, Van Nostrand and Reinhold, New York (1967).

23. R. R. COVEYOU, V. R. CAIN, and K. J. YOST, "Adjoint and Importance in Monte Carlo Application," *Nucl. Sci. Eng.*, **27**, 219 (1967).

24. M. H. KALOS, "Importance Sampling in Monte Carlo Shielding Calculations: I. Neutron Penetration Through Thick Hydrogen Slabs," *Nucl. Sci. Eng.*, **16**, 227 (1963).

25. V. R. CAIN, "Application of $S_N$ Adjoint Flux Calculations to Monte Carlo Biasing," *Trans. Am. Nucl. Soc.*, **10**, 399 (1967).

26. G. E. WHITESIDES, "Adjoint Biasing in Monte Carlo Criticality Calculations," *Trans. Am. Nucl. Soc.*, **11**, 159 (1968).

27. J. S. TANG, P. N. STEVENS, and T. J. HOFFMAN, "Methods of Monte Carlo Biasing Using Two-Dimensional Discrete Ordinates Adjoint Flux," ORNL/TM-5414, Oak Ridge National Laboratory (1976).

28. J. S. TANG and T. J. HOFFMAN, "Monte Carlo Shielding Analyses Using an Automated Biasing Procedure," *Nucl. Sci. Eng.*, **99**, 329 (1988).

29. P. C. MILLER, G. A. WRIGHT, G. B. BOYLE, and S. W. POWER, "The Use of an Inbuilt Importance Generator for Acceleration of the Monte Carlo Code MCBEND," *Proc. Int. Conf.*

*Physics of Reactor Operation, Design and Computation*, Marseille, France, April 23–26, 1990, p. 124 (1990).

30. S. CHUCAS and M. GRIMSTONE, "The Acceleration Techniques Used in the Monte Carlo Code MCBEND," *Proc. 8th Int. Conf. Radiation Shielding*, Arlington, Texas, April 24–28, 1994, Vol. 2, p. 1126, American Nuclear Society (1994).

31. M. W. MICKAEL, "Importance Estimation in Monte Carlo Modelling of Neutron and Photon Transport," *Nucl. Geophys.*, **6**, *3*, 341 (1992).

32. M. W. MICKAEL, "A Fast, Automated, Semideterministic Weight Windows Generator for MCNP," *Nucl. Sci. Eng.*, **119**, 34 (1995).

33. J. C. WAGNER and A. HAGHIGHAT, "Deterministic Adjoint Functions for Biasing Monte Carlo Reactor Cavity Dosimetry Calculations," *Trans. Am. Nucl. Soc.*, **73**, 432 (1995).

34. J. C. WAGNER and A. HAGHIGHAT, "Application of the Discrete Ordinates Adjoint Function to Accelerate Monte Carlo Reactor Cavity Dosimetry Calculations," *Proc. Topl. Mtg. Radiation Protection & Shielding*, No. Falmouth, Massachusetts, April 21–25, 1996, Vol. 1, p. 345, American Nuclear Society (1996).

35. J. C. WAGNER and A. HAGHIGHAT, "Acceleration of Monte Carlo Reactor Cavity Dosimetry Calculations with the Discrete Ordinates Adjoint Function," *Proc. 9th Int. Symp. Reactor Dosimetry*, Prague, Czech Republic, September 2–6, 1996.

36. S. A. TURNER, "Automatic Variance Reduction for Monte Carlo Simulations via the Local Importance Function Transform," LA-13119-T, Los Alamos National Laboratory (1996).

37. K. A. VAN RIPER et al., "AVATAR—Automatic Variance Reduction in Monte Carlo Calculations," *Proc. Joint Int. Conf. Mathematical Methods and Supercomputing for Nuclear Applications*, Saratoga Springs, New York, October 6–10, 1997, American Nuclear Society.

38. K. NOACK, "Efficiency and Reliability in Deep-Penetration Monte Carlo Calculations," *Ann. Nucl. Energy*, **18**, 309 (1991).

39. W. A. RHOADES and R. L. CHILDS, "The DORT Two-Dimensional Discrete Ordinates Transport Code System," CCC-484, ORNL-RSICC, Oak Ridge National Laboratory (1989).

40. D. E. KNUTH, *The Art of Computer Programming*, 2nd ed., Addison-Wesley, Reading, Massachusetts (1973).

41. G. L. SIMMONS and R. ROUSSIN, "SAILOR—A Coupled Cross-Section Library for Light Water Reactors," DLC-76, ORNL-RSICC, Oak Ridge National Laboratory (1983).

42. J. C. WAGNER, A. HAGHIGHAT, B. G. PETROVIC, and H. L. HANSHAW, "Benchmarking of Synthesized 3-D $S_N$ Transport Methods for Pressure Vessel Fluence Calculations with Monte Carlo," *Proc. Int. Conf. Mathematics and Computations, Reactor Physics, and Environmental Analyses*, Portland, Oregon, April 30–May 4, 1995, Vol. 2, p. 1214, American Nuclear Society (1995).

43. J. C. WAGNER, A. HAGHIGHAT, and B. G. PETROVIC, "Monte Carlo Transport Calculations and Analysis for Reactor Pressure Vessel Neutron Fluence," *Nucl. Technol.*, **114**, 373 (1996).

44. B. PETROVIC, J. C. WAGNER, and A. HAGHIGHAT, "Verification of Improved Synthesized 3-D $S_N$ and Monte Carlo Methods for Pressure Vessel Fast Neutron Fluence Calculations," *Proc. Joint Int. Conf. Mathematical Methods and Supercomputing for Nuclear Applications*, Saratoga Springs, New York, October 6–10, 1997, American Nuclear Society.

45. A. HAGHIGHAT, M. MAHGEREFTEH, and B. G. PETROVIC, "Evaluation of the Uncertainties in the Source Distribution for Pressure Vessel Neutron Fluence Calculations," *Nucl. Technol.*, **109**, 54 (1995).